

WOODEN DISK COMBUSTION FOR SPOT FIRE SPREAD

by

J.P. Woycheese
Center for Firesafety Studies
Worcester Polytechnic Institute
Worcester, MA 01609-2280, USA

Reprinted from the Interscience Communications Ltd.; Building Research Establishment; National Fire Protection Association; National Institute of Standards and Technology; Society of Fire Protection Engineers; and Swedish National Testing and Research Institute. Interflam '2001. International Interflam Conference, 9th Proceedings. Volume 1. September 17-19,2001, Edinburgh, Scotland, Interscience Communications Ltd., London, England, 101-112 pp, 2001.

NOTE: This paper is a contribution of the National Institute of Standards and Technology and is not subject to copyright.



NIST

National Institute of Standards and Technology
Technology Administration, U.S. Department of Commerce

WOODEN DISK COMBUSTION FOR SPOT FIRE SPREAD

J. P. Woycheese

Center for Firesafety Studies, Worcester Polytechnic Institute

ABSTRACT

More than 500 experiments were conducted to explore the effects of wood type, sample size, relative velocity, and grain orientation on the combustion of wooden disk-shaped brands. Two combustion phenomena groups, complete combustion and self-extinction, were observed among the seven species examined, with those species having densities greater than 300 kg/m^3 primarily forming the latter group. Grain orientation was also found to have significant effect on brand lifetime, although the variation for a particular brand size and velocity could vary by more than 50%.

1 INTRODUCTION

Spot ignition by burning brands launched ahead of the flame front of large fires is an important mechanism for fire spread in post-earthquake and urban/wildland intermix conflagrations. Although the problem of lofting and transport of burning brands in forest fires has received considerable attention [1-8], little research has been done to quantify the transport of brands from burning structures. Brand-initiated fires are of particular importance in "urban/wildland intermix" regions, which are areas of measurable girth and depth, with structures in natural surroundings with copious vegetation nearby.

Brand propagation from large fires is a complex problem. Important issues include time-dependent wind and plume velocity fields; brand size and shape distributions; wood combustion rates; and terrain effects. Previous research has concentrated on spherical and cylindrical brands [1-8] because the focus has been on wildland and forest fires, where these shapes will dominate the brand distributions. For urban/wildland intermix fires, however, disk brands are likely to play a more significant role, due to the availability of thin, flat shingles from which disks can be derived [9] and to the superior lofting ability of disk-shaped brands. This research was undertaken to extend the existing fire propagation models and to quantify some of the brand parameters to enable better computer simulation of brand-driven conflagrations.

Recently, a number of large, costly fires have occurred across the United States: the Santa Barbara "Paint" fire of 1990, the Oakland Hills' Fire of 1991, the Southern California and Florida Fires of the late 1990's, and the Los Alamos Fire of 2000, to name a few. The 20 October 1991 Oakland Hills Fire, which caused more than \$1 billion in damages [10], is a good example of a brand-propagated fire in an urban/wildland intermix region, with propagation by flaming brands hundreds of meters ahead of the fire front [10]. Sapsis has developed data on the Oakland Hills' Fire, from eyewitness and emergency crew accounts and from emergency phone call logs, which data clearly show significant propagation by spot fires more than 1000m from the main fire front during the initial hours of the conflagration.

One eyewitness observed a flying, burning shingle from an unusual platform: an air tanker flying at an altitude of two thousand feet [11].

Although there has been significant analytical research into the lofting and propagation of firebrands, especially with regard to large forest fires, there is a decided lack of experimental data available on the combustion of wood under forced-flow conditions. Tarifa et al. [5, 6] conducted the premiere experimental work to date. (See [7] for a more detailed synopsis of brand combustion research.) A number of analytical models have been based on this data, which focused primarily on spherical and cylindrical brands, as is appropriate for large forest fires. It can be argued, however, that for urban/wildland intermix fires, disk brands are likely to play a more significant role: thin, flat shingles from which disks can be derived are available in prodigious amounts, while the disk-shaped brands formed therefrom have superior propagation ability [7]. In addition, the terminal velocity for disk brands is substantially smaller than that for cylinders and spheres of the same diameter, resulting in greater risk of spot fire propagation by disk brands.

The remainder of this paper will provide information on the experiments conducted into disk brand combustion. The next section, Experimental Setup and Observations, presents an overview of the experimental process, general observations, and lessons experienced hereby. The Results section provides experimental outcomes for samples that either burned to completion or that self-extinguished, for a range of wood species, sample sizes, and relative velocities. The Conclusions section provides a synopsis of the resolutions construed from the experimental data.

2 EXPERIMENTAL SETUP AND OBSERVATIONS

This research is intended to complement the work conducted by Tarifa by providing experimental data for the combustion of disk-shaped wooden brands in forced flow. Seven wood species were tested: Balsa (*Ochroma Pyramidale*), Western Red Cedar (*Thuja Plicata*), Douglas Fir (*Pseudotsuga Taxifolia*), Red Oak (*Quercus Borealis*), Honduras Mahogany (*Sweitenia Macrophylla*), Redwood (*Sequoia Sempervirens*), and Walnut (*Juglans Nigra*). The latter three types were examined less rigorously in this work, so these species will be analyzed together. The Balsa samples had a bimodal density distribution that was exhibited between different wood pieces. The growth rates of Balsa are highly dependent on the availability of water; resulting densities can vary from 60 to 400 kg/m³ [12]. For this research, samples with densities, from 65 to 100 kg/m³ (air-dry), were classified as Light Balsa, while those from 135 to 160 kg/m³ were called Balsa. Red Oak likewise had a bimodal distribution, with peaks at 690 and 780 kg/m³. In this case, however, there was a natural segregation with sample diameter, so Red Oak samples were not split into sub-species.

Three sizes of samples were produced: small, large, and thin. Nominally, small disks were 25 mm in diameter and 8.3 mm thick (1:3 length-to-diameter ratio), large disks were 50 mm by 17 mm (1:3), and thin disks were 50 mm by 5.5 mm (1:9). Not all sizes were available for all wood types. The average densities, by wood type and sample size, are provided in Table 1, below.

Videographic images and gravimetric measurements were developed for combusting wooden disks in forced flow. The effect of wood type, sample size, and wood grain orientation was determined for a variety of forced-flow velocities.

Table 1: Average Wood Density by Type and Sample Size

Wood Type	Average Density		
	Small	Large	Thin
Light Balsa		80	
Balsa	145	145	142
Western Red Cedar	269		
Redwood	297		
Honduras Mahogany	466		
Douglas Fir	568	597	533
Walnut	639		
Red Oak	656	750	760

2.1 Sample Preparation

Identical samples, of a variety of wood types, were fabricated with an emphasis on minimal dimensional and orientational variabilities. Where possible, samples were derived from commercial wooden dowels of appropriate diameter, which were cut perpendicular to the axis of symmetry to give disks of the desired proportions. When dowels were unavailable or of prohibitive cost, lumber was cut into parallelepipeds either 38 mm (1.5") or 64 mm (2.5") square and 600 mm (24") long. These sawn boards were turned on a lathe to the desired diameter and cut into disks. The surface roughness of the disks was regulated for neither commercial nor manufactured dowels. The resultant disks had end grain exposed on the flat surfaces.

Samples were weighed using a torsion-balance scale and measured with calipers. An 0-80, 1"-long screw was passed through a hole drilled axially through the center and fixed in place with a ceramic glue, which could withstand temperatures up to 1540°C. Screw and glue masses were deducted from oven-dry and post-experimental values to determine organic mass. Samples were dried in an oven, kept between 101 and 105°C to remove moisture per ASTM 4442 [13]. The time required to dry the sample depended on wood type, diameter, and ratio, but mass for large fir samples stabilized to within 1% after approximately three hours, and remained at that mass for at least 60 hours. Balsa dried in one to two hours, while oak dried within eight. Samples remained in the oven for a minimum of eight to twelve hours, dependent upon the above parameters, although the majority was dried for 24 hours or more.

The samples were weighed and measured to determine oven-dry characteristics. Due to hygroscopic concerns (absorption of moisture from the air), the ignition process commenced within ten minutes of sample removal from the oven. The sample moisture content rarely exceeded 0.5% prior to ignition.

2.2 Ignition Method

Several ignition processes were examined in an effort to determine the method that provided the most reproducible results. Tarifa, et al., [5, 6] used a blowtorch on the sample in the wind tunnel for a specified time period. This method was found to have low reproducibility for larger, 50-mm-diameter samples and left less than 30% of the original mass after the ignition process for 25-mm-diameter Western Red Cedar disks. Accelerants were used, both with and without the blowtorch, with similar, unrepeatable results.

A radiant heater with a spark ignition was found to be the ignition method with the

best repeatability. The samples were pre-heated using a radiant heater created by wrapping chromium wire around a ceramic core. The heater was maintained at a temperature of 840 to 870 °C by limiting the voltage applied across the chromium with a variac. A high-frequency spark generator was activated at a set time during the heating process, providing the energy required to ignite the samples.

The time of activation for each wood type was determined experimentally and resulted in uniform ignition on the fully exposed surface. This time varies with kpc, [7]. Activating the spark generator prior to this time resulted in either significant ignition delay or samples that were not uniformly ignited. In the latter case, ignition occurred in the immediate vicinity of the spark, but the flame did not propagate over the entire face of the brand, as occurred during acceptable (i.e., repeatable) ignitions. Poorly ignited samples quickly self-extinguished if subjected to forced flow. Spark generation after the experimentally determined time resulted in unnecessary sample degeneration. Mass loss due to pyrolysis occurs during the pre-heating process; minimum ignition time is desired to provide maximum material for the experiment.

2.3 Experimental Procedure

Once the ignition process was complete, the apparatus holding the burning samples was mounted in the wind tunnel, which was started and accelerated to the desired speed. The test section had high-temperature windows in three sides, which enabled the observation of significant events and the simultaneous videographic recording of the experiment from two perpendicular directions.

2.4 Post-Experiment Processes

Although the majority of samples were allowed to burn to self-extinction (including complete combustion), some few samples were removed at specific times and quenched with CO₂ to enable the development of time-dependent combustion data. Upon cessation of combustion, samples were weighed and, when of regular shape, measured by calipers prior to immersion in liquid paraffin wax. Paraffin wax, which was maintained above its melting point in a specially designed open-top container, sealed the pores of the samples so that their volume could be measured using the displacement method described in ASTM 2395-93 (Method B) [14]. For fractured samples, the volume of each piece was determined individually and combined to determine the sample volume.

3 Results

More than 500 experiments were conducted over a period of approximately ten months. The effects of wood type, sample diameter and thickness, relative velocity, and grain orientation on combustion times and sample properties were explored in the course of these experiments.

3.1 General Observations

There were three distinct combustion processes observed during these experiments: flaming, surface, and sub-surface combustion. The first two processes were the more common, occurring to varying degree with every sample tested. Sub-surface combustion was very rare, with only a few recorded instances.

Upon sample ignition, an enveloping flame developed that covered the sample face – the side that was closest to the heater during pre-ignition and that was placed upwind in the wind tunnel – as shown in the left-most images in Fig. 1. This figure provides typical time-lapse images of Douglas Fir and Western Red Cedar disks. Visible through this enveloping or face flame, after a short start-up time, was an area involved in surface combustion. The

surface combustion was most significant at the edges of the face, and would begin to involve material toward the center of the sample if the face flame remained stable for sufficient time. This stability was dependent on sample species, size, orientation, and both the steady velocity supplied by the wind tunnel and the tunnel acceleration from rest to the desired velocity. Typically, the face flame would remain stable to approximately 2 m/s if the acceleration was less than 0.7 m/s^2 . This stability velocity decreased to slightly more than 1 m/s for accelerations of 2 m/s^2 . Face flame longevity was dependent on velocity, wood type, and sample size. Decreasing velocity, thickness, or diameter, or increasing density, resulted in longer face flame times.

Concurrent with, and often outlasting, flaming combustion, surface combustion occurred first along the facial edges of the samples and was the dominant combustion process for less dense materials like cedar and balsa. While surface combustion for oak and fir samples self-extinguished without a nearby, supporting, flame (see the images for $t=40 \text{ s}$ in Fig. 1), the lighter wood types burned to completion due to the persistence of the surface burning. Figure 1 also clearly shows the difference between two types of materials; the more dense Douglas Fir has a longer lasting flame, but ultimately self-extinguishes with significant mass remaining. The flaming combustion of the Western Red Cedar sample, by comparison, terminates early in the sample lifetime, but surface combustion develops over the entire sample. The regression rate due to surface combustion was affected by the material density; Balsa samples burned to completion much faster than their Western Red Cedar counterparts,

Two different combustion phenomena were discovered in the course of these experiments. One, which primarily affected Balsa, Western Red Cedar, and Honduras Mahogany samples, led to the complete combustion of these specimens for a variety of sizes and velocities. The second, for Douglas Fir, Redwood, and Red Oak, generally induced self-extinguishment with significant residual mass, volume, and density. Density appears to have a significant role, as the samples with the lowest density burned to completion with more regularity than their counterparts. One early indication of mechanism is the spread of surface combustion on the sample face; samples with complete facial surface combustion invariably burned to completion, while only a very few others completely combusted. Finally, increasing velocity strongly decreased combustion times and increased post-experiment mass and density.

Flames lasted longer at lower speeds, while surface combustion increased with increasing velocity. Even the lower-density wood types, however, required that flaming combustion persist until surface combustion could be established, although this could be as short as a few seconds. Therefore, optimal conditions for brand transport require low wind speeds subsequent to brand ignition, with increased velocities after the surface combustion becomes established. Most brand propagation models to date, however, utilize high initial velocities that decrease with time.

3.2 Grain Orientation

The majority of experiments conducted for this research oriented the sample's wood grain so that it was parallel to the wind stream, exposing the end grain. It was found that grain orientation plays a significant role in the combustion process of wood in a forced flow. The ignition and subsequent combustion of cross-grain experiments – those where the grain was perpendicular to the wind stream – was extremely variable (see Fig. 2), with irregular flaming and surface combustion that never resulted in sample consummation.

For experiments with a cross-grain face normal to the relative velocity, flaming combustion was concentrated on the edges of the sample, at the end grain. Combustion on

the face, both flaming and surface, was spotty and short-lived; and there was little, if any, combustion on the rear surface. Figure 2 provides a comparison of sample extinction times with grain orientation as a function of relative velocity for 25-mm-diameter cedar disks with a 1:3 nominal length-to-diameter ratio. All end-grain samples burned to completion for speeds less than 4 m/s, while none of the cross-grain samples did so. The combination of complete and incomplete combustion for end-grain samples at 4 m/s resulted in the larger variability at that speed, as small portions of the latter samples would burn for long time periods.

3.3 Velocity and Density Effects

Relative velocity and initial brand size and density play varying roles in both brand lifetime and the rate and degree to which mass is lost before self-extinction. In general, as may be expected, lifetimes increase with density and decrease with velocity. (See Fig. 3.) Larger disks of the same length-to-diameter ratio usually outlast their smaller brethren, Red Oak at the lowest velocity, however, does not follow this rule, as both small and thin samples will burn to completion – no residual mass – and the larger samples will self-extinguish with significant residual mass; as a result, the small Red Oak disks outlast the larger. Also seen from Fig. 3 are the relatively short lifetimes of thin disks at all speeds, with the exception (again) of Red Oak.

For small samples that do not completely combust, a group that includes Redwood, Douglas Fir, Walnut, and Red Oak (above 1 m/s), the average residual mass tends to increase with velocity. This data is shown in Fig. 4 as a function of the average oven-dry sample density provided in Table 1, and in Fig. 5 as a function of the brand lifetime. Similarly, for large samples that self-extinguish, the residual values generally increases with velocity for all species. Thin disks, however, do not exhibit dependence on velocity for residual mass and density. The average residual mass for samples that burn to completion – Light Balsa, Balsa, Western Red Cedar, and Honduras Mahogany – have no residual mass by definition.

It is interesting to note, from Fig. 5, that the average residual mass for all wood types does not exceed

$$\text{ARM} = (-0.125 \cdot \text{BET} + 100)\% \quad (1)$$

where **ARM** is the average residual mass in percent and **BET** is the time of brand extinction in seconds. This seems to indicate that there is a minimum mass loss rate for all of the wood types examined, regardless of the time of combustion.

It can be seen in Fig. 5 that the extinction times for small disks depend both on sample density and combustion characteristics; samples are collected into groups that did and did not burn to completion. The extinction times for each group generally decreased with velocity. There was overlap between the two, as some light, completely combusting specimens would outlast those for more dense, self-extinguishing species. The sample lifetimes for Red Oak were more than double those for Douglas Fir. Brand lifetimes for large samples do not appear to be a function of its density, but typically are affected by velocity. Sample lifetimes for thin disks of all species are seen to decrease with increasing velocity. The Red Oak samples far outlast those of the other species, an event that was not predicted from the other extinction comparisons for this size. Balsa and Douglas Fir have comparable lifetimes, although the former burn to completion and the latter do not.

Glowing for the more dense woods is a smaller fraction of the combustion process at higher velocities; hence, at lower velocities where small, protected areas of glowing combustion can exist for long periods, the total combustion time of Douglas fir exceeds that for the woods that burn to completion. At 2 m/s, Red Oak samples had small, persistent areas

of glowing combustion on the downwind side of the samples.

One Douglas Fir sample developed an internal combustion process that eventually fractured the sample. The results for the 1 m/s case are skewed as a result, because the glowing combustion section for that sample, at 360 seconds, was as long as the complete combustion of other samples and was an anomaly was not repeated with the process used for these experiments.

The average residual density is provided as a function of brand lifetime in Fig. 6. The density was determined from measured mass and displaced volume values. Two symbols on Fig. 5 do not have corresponding values on Fig. 6, as the displaced volume was not available for the Honduras Mahogany or Walnut samples. The decrease in density from 100% indicates that a significant fraction of the sample is made of char, rather than virgin or near-virgin wood. This determination is strengthened by the fact that the density of the larger samples decreases with increased sample lifetime. The samples in the highest velocity stream extinguished the most rapidly due to a removal of pyrolyzed material prior to combustion combined with the convective cooling; these samples were observed to have very thin layers of discolored wood, below which could be found virgin material. The longer burning samples, however, typically became carbonaceous char of varying density throughout.

3.4 Temporal Effects

As discussed briefly in Experimental Setup and Observations, a number of experiments were halted prior to sample self-extinguishment by submersing the burning samples in an atmosphere of CO₂. These experiments enabled the construction of average intra-experimental sample data, as provided in Figs. 7 and 8. In Fig. 7, the ordinate was developed by dividing the measured post-experimental mass by the average post-experimental mass of samples extinguished after the ignition process. Similarly, the ordinate for Fig. 8 is the ratio of the measured post-experimental mass divided by the displacement volume (post-experimental density) to the average post-experimental density for samples extinguished immediately after ignition. For both figures, the abscissa is the ratio of the sample extinguishment time to the average time for self-extinction for that size and species, as determined in prior experiments detailed previously. Dimensional values can be found in Appendix B of Ref [7]. Note that a single sample can burn for greater than 100% of the average extinction time on which the abscissa is based. For a relative velocity of 2 m/s, the mass loss curves generally decrease with oven-dry density. Western Red Cedar and Balsa curves approach each other after approximately 25% of average sample lifetime.

The effects of sample size on mass history curves are also visible in Fig. 7 for Douglas Fir disks. Both small (25-mm dia., 1:3 l:d) and large (50-mm dia., 1:3 l:d) samples were tested at 2 m/s. As for the previous section, residual values are plotted against fractional extinction times to enable direct comparison of dissimilar dimensional values. The small samples lose mass at a faster rate and to a larger degree than the large samples.

Primary mass and density loss for species that burn to completion, like Western Red Cedar and Balsa, occurs early in the combustion process. Corresponding losses for self-extinguishing species, such as Douglas Fir, tended to be slower and more constant. Thus, combustion characteristics could be determined from the residual curves alone, as samples that burn to completion generally have dominant surface combustion.

The density for large Douglas Fir samples, as shown in Fig. 8, changes very little from the average value after the ignition process. This indicates that mass loss is closely tracked by volume regression for this case. For small Douglas Fir samples, the density decreases slightly, indicating a larger fraction of carbonaceous char. The values for small

Balsa and Western red Cedar are the most telling, however, as it can be seen that the large drop in mass shown in Fig. 7 is accompanied by little change in volume (resulting in a large change in density). Thus, the aerodynamic properties of these two species will change accordingly.

4 CONCLUSIONS

This work is intended to provide a better understanding of the mechanics and properties of wooden brands during lofting above and propagation from large-scale fires. The experiments expanded forced-flow combustion data to include disk-shaped brands, enabling the extension of existing propagation models and the quantification of some of the brand parameters to enable better computer simulation of such conflagrations.

More than 500 experiments were conducted over a period of approximately ten months, including a number of exploratory trials. These latter experiments established the wood-specific spark generation times used in the ignition process, as well as ascertaining the best ignition process. The effects of wood type; sample diameter, thickness, and grain orientation; and relative velocity on combustion times and sample properties were explored in the course of these experiments. The majority of tests were conducted on samples with the end grain exposed to the oncoming wind.

Seven wood species were tested: Balsa (*Ochroma Pyramidale*), Western Red Cedar (*Thuja Plicata*), Douglas Fir (*Pseudotsuga Taxfolia*), Red Oak (*Quercus Borealis*), Honduras Mahogany (*Sweitenia Macrophylla*), Redwood (*Sequoia Sempervirens*), and Walnut (*Juglans Nigra*). The Balsa samples had a bimodal density distribution, due to differing growth rates, and were thus split into two subgroups. Three sizes of samples were produced: small, large, and thin. Nominally, small disks were 25 mm in diameter and 8.3 mm thick (1:3 length-to-diameter ratio), large disks were 50 mm by 17 mm (1:3), and thin disks were 50 mm by 5.5 mm (1:9). Not all sizes were available for all wood types.

For the species examined, two combustion phenomena were observed. Some of the species burned to completion at nearly all speeds, while the other group – all of which had a density above 300 kg/m^3 – burned out with significant mass remaining. Surface or glowing combustion was the dominant mechanism for the former group, while the majority of mass loss for the latter stemmed from flaming combustion.

It was also found that the species that burned to completion lost 40% or more of their mass in the first decade, and 90% in the first half of their lifetime. The density for these samples decreased significantly over time, due to a much lower volume regression rate. As a result, brands formed from Balsa, Western Red Cedar, Honduras Mahogany, or similar species are likely to propagate greater distances than those generated from Douglas Fir, Red Oak, Walnut, or Redwood. The dependence of the latter group on flaming combustion for viability also indicates a lesser ability for ignition upon deposition.

Although few experiments were conducted on cross-grain samples, such as disks cut from shakes and shingles, it appears that their slow relative mass loss, due to spotty surface combustion along the brand edge, may increase the propagation distance by increasing the brand lifetime. When initial combustion was sparse, a small, persistent combustion area would occasionally form near the edge of the sample. These runs would exhibit significantly longer lifetimes than was normal for the size and configuration. It is likely that, in a fire environment, such disks, partially ignited on their edges, would propagate the farthest. Large numbers of long-duration, partially ignited disks would pose a significant risk to spot fire propagation.

5 Future Work

More study is required before a fully viable combustion model can be developed for accurate prediction of probability distributions for spot fire distances. Wood combustion is an extremely complex phenomenon [15,16] with many facets yet to be explored. Of particular interest to the issue of brand lofting and combustion, however, are the aerodynamic and gravimetric forces on brands in a variety of wind conditions and orientations. These are necessary for inclusion of brand transport in both large-scale fire [17] and large-eddy simulation models [18-19]. The resolution of lift and drag forces on combusting disks at different angles of attack, for example, would enable better predictions of propagation distances. Similarly, a better understanding of tumbling effects on brand combustion and aerodynamic forces is desirable. Although some research has been conducted on the combustion rate of burning, tumbling brands and on the forces on tumbling, noncombusting wood pieces [20-25], little has been done to quantify the combination of these effects. A more thorough examination of the combustion characteristics of cross-grain disks, expanding on the work conducted here, is also in order.

6 Acknowledgements

The author is grateful for the financial support provided by the Building and Fire Research Laboratory of the National Institute of Standards and Technology, U.S.D.O.C., under Grant No. 60NANB8D0094. The author is indebted to Patrick J. Pagni for his guidance and support.

6 References

1. Muraszew, A., "Firebrand Phenomena," *Aerospace Report No. ATR - 74 (8165 -01) - 1*, The Aerospace Corporation, El Segundo, 1974.
2. Muraszew, A., Fedele, J.B., and Kuby, W.C., "Firebrand Investigation," *Aerospace Report ATR-75 (7470) - 1*, The Aerospace Corp., El Segundo, CA, 1975.
3. Albini, F.A., "Spot Fire Distance From Burning Trees: A Predictive Model," *General Technical Report No. INT - 56*, USDA Forest Service Intermountain Forest and Range Experiment Station, Ogden, UT, 1979.
4. Albini, F.A., "Potential Spotting Distance from Wind-Driven Surface Fires," *USDA Forest Service Research Paper ZNT-309*, USDA, 1983.
5. Tarifa, C.S., del Notario, P.P., and Moreno, F.G., "On the Flight Paths and Lifetimes of Burning Particles of Wood," *Tenth Symposium (International) on Combustion*, 1021-1037, The Combustion Institute, 1965.
6. Tarifa, C.S., del Notario, P.P., Moreno, F.G., and Villa, A.R., "Transport and Combustion of Firebrands," *Final Report of Grants FG-SP-114 and FG-SP-146, Vol. 2*, USDA, Madrid, 1967.
7. Woycheese, J.P., "Brand Lofting and Propagation from Large-Scale Fires," *Ph.D. Dissertation*, University of California, Berkeley, 2000.
8. Fernandez-Pello, A.C., "An Analysis of the Forced Convective Burning of a Combustible Particle," *Combustion Science and Technology*, v. 28, 305-313, 1982.
9. Waterman, T.E., "Experimental Study of Firebrand Generation," *Final Technical Report: Project J6130*, IIT Research Institute, Chicago, IL, 1969.
10. Pagni, P.J., "Causes of the 20th October 1991 Oakland Hills Conflagration," *Fire Safety Journal*, 21:4, 331-340, 1993.
11. Sullivan, M., *Firestorm! : The Story of the 1991 East Bay Fire in Berkeley*, p. 36, City of Berkeley, Berkeley, CA, 1993.
12. Ashmore, H.S., ed., "Balsa," *Encyclopaedia Britannica*, Vol. 2, William Benton, Chicago, 1961.
13. "D 4442-92: Standard Test Methods for Direct Moisture Content Measurement of Wood and Wood-Base Materials," *Annual Book of ASTM Standards*, v. 4.10, American Society for Testing and Materials, West Conshohocken, PA, 489-493, 1999.
14. "D 2395-93: Standard Test Methods for Specific Gravity of Wood and Wood-Based Materials," *Annual Book of ASTM Standards*, v. 4.10, American Society for Testing and Materials, PA, West Conshohocken, 350-357, 1999.
15. Di Blasi, C., "Modeling and Simulation of Combustion Processes of Charring and Non-Charring Solid Fuels," *Progress in Energy and Combustion Science*, 19:1, 71-104, 1993.

16. Roberts, A.F., "Problems Associated with the Theoretical Analysis of the Burning of Wood," *Thirteenth Symposium (International) on Combustion*, 893-903, The Combustion Institute, 1971.
17. Linn, R.R., Bosset, J.E., Harlow, F.H., Reisner, J.M., and Smith, S., "Studying Complex Wildfire Behaviors Using FJRETEC," *Preprints of Third Symposium on Forest and Fire Meteorology*, AMS 80th Annual Meeting, Long Beach, CA, 15-20,2000.
18. McGrattan, K.B., Ferek, R.J., and Uthe, E.E., "Smoke Plume Trajectory from In Situ Burning of Crude Oil – Field Experiments," *Proceedings of the First International Conference on Fire Research and Engineering*, ed. D. Peter Lund, 47-52, Society of Fire Protection Engineers, Orlando, FL, 1995.
19. McGrattan, K.B., Baum, H.R., Rhem, R.G., Hamins, A., Forney, G.P., "Fire Dynamics Simulator – Technical Reference Guide," *NISTIR 6467*, National Institute of Standards and Technology, Gaithersburg, MD, 2000.
20. Ragland, K.W., Mason, M.A., and Simmons, W.W., "Effect of Tumbling and Burning on the Drag of Bluff Objects," *Journal of Fluids Engineering*, v. 105, 174-178, June 1983.
21. Marchildon, E.K., Clamen, A., and Gauvin, W.H., "Oscillatory Motion of Freely Falling Disks," *Physics of Fluids*, v. 7, 2018-2019, 1964.
22. Marchildon, E.K., Clamen, A., and Gauvin, W.H., "Drag and Oscillatory Motion of Freely Falling Cylindrical Particles," *Canadian Journal of Chemical Engineering*, **42**:4, 178-182, 1964.
23. Willmarth, W.W., Hawk, N.E., and Harvey, R.L., "Steady and Unsteady Motions and Wakes of Freely Falling Disks," *Physics of Fluids*, **7**:2, 197-208, 1964.
24. Crowe, C.T., Nicholls, J.A., and Morrison, R.B., "Drag Coefficients of Inert and Burning Particles Accelerating in Gas Streams," *Ninth Symposium (International) on Combustion*, 395-406, The Combustion Institute, New York, 1962.
25. Stewart, R.E., and List, R., "Gyrational Motion of Disks During Free-Fall," *Physics of Fluids*, **26**:4, 920-927, April 1983.

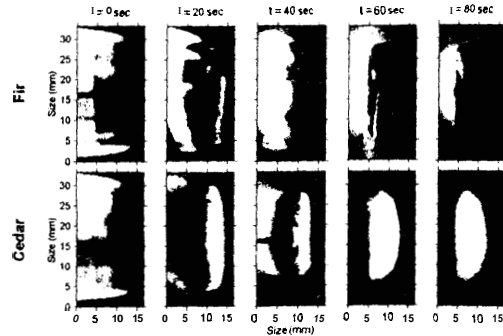


Figure 1: Comparison of combustion images for Douglas Fir and Western Red Cedar samples in a 1.8 m/s relative velocity. Both pieces were 25 mm in diameter and 8 mm thick. The fir extinguished at 90 s with 50% residual mass. The cedar burned to completion (zero residual mass) after 210 s. White coloring on the surface of the samples denotes areas of surface combustion.

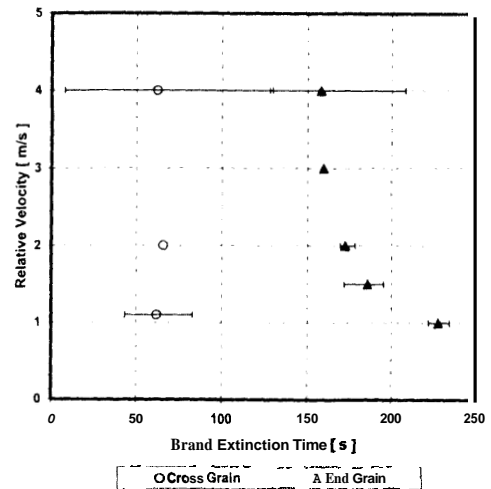


Figure 2: Sample extinction times for 25-mm-diameter cedar disks in cross- and end-grain orientation as a function of relative velocity. End-grain samples burned to completion at speeds less than 4 m/s, with regular flaming and surface combustion, unlike their cross-grain counterparts.

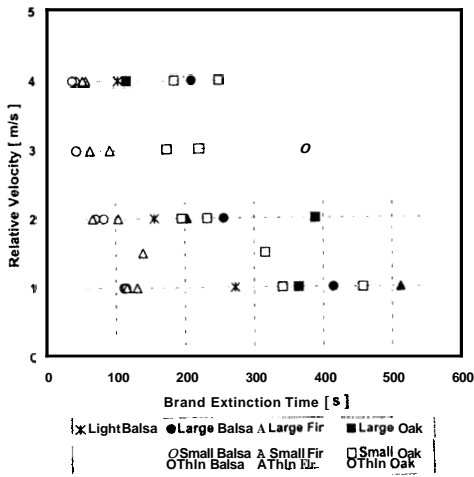


Figure 3: Comparison of average sample lifetimes as functions of velocity. Lifetimes generally increased with density and decreased with velocity. Small disks are 25 mm in diameter and 8 mm thick, large disks are 50 mm by 16 mm, and thin disks are 50 mm by 8 mm.

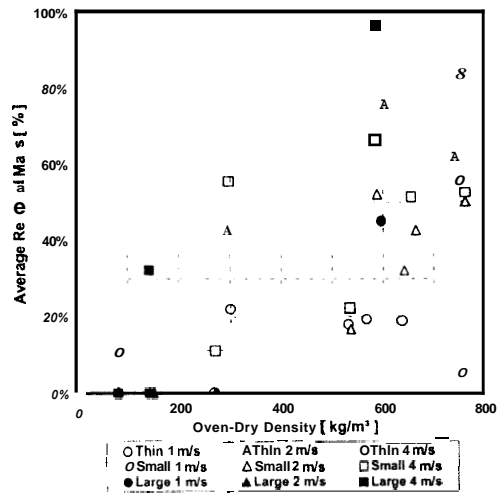


Figure 4: Average residual mass as a function of oven-dry density for disks of all species and sizes at 1, 2 and 4 m/s. Those found along the ordinate have burned to completion.

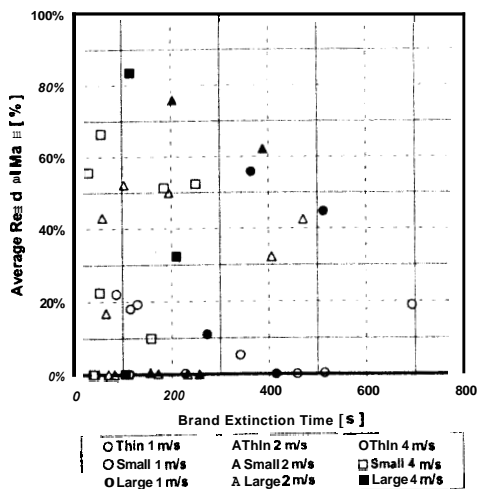


Figure 5: Average residual mass as a function of brand lifetime for disks of all species and sizes at 1, 2 and 4 m/s. All samples were allowed to burn to self-extinction; those along the abscissa have burned to completion (no residual mass).

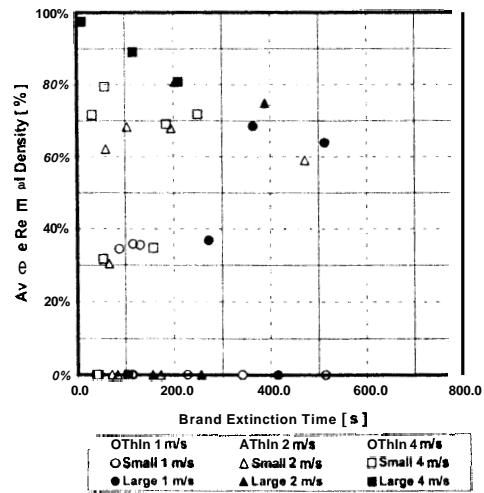


Figure 6: Average residual density as a function of brand lifetime for disks of all species and sizes at 1, 2, and 4 m/s. All samples burned to self-extinction. A density of "0" indicates that there was no residual mass.

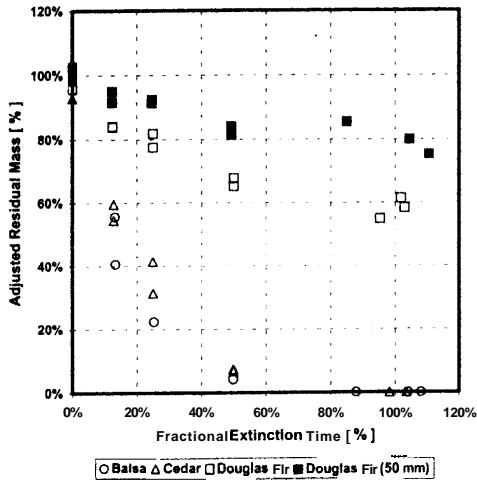


Figure 7: Comparison of adjusted residual mass (ratio of post-experimental mass to the average for samples extinguished immediately after ignition) for noted wood types in a 2-m/s relative velocity as a function of fractional extinction time (extinguished to average wood- and size-specific extinction time). Open symbols denote small samples; solid symbols signify large disks. Mass loss curves decrease with initial density.

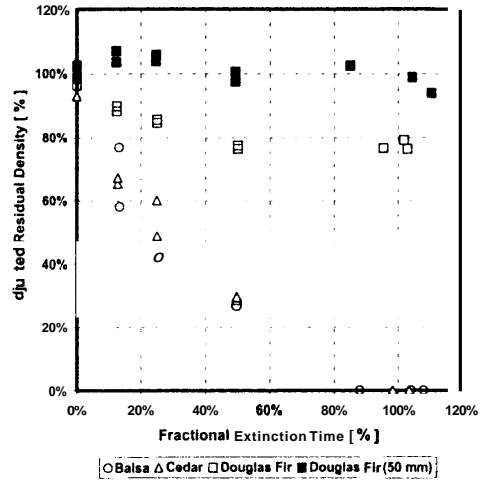


Figure 8: Comparison of adjusted residual density (ratio of post-experimental density to the average for samples extinguished immediately after ignition) for noted wood types in a 2-m/s relative velocity as a function of fractional extinction time. Open symbols denote small samples; solid symbols signify large disks. Density for large fir disks is nearly constant, indicating that most wood is virgin or nearly so. **Balsa** and cedar curves decrease rapidly; a significant fraction of the sample becomes char.